Catal Lett (2010) 134:169–174
DOI 10.1007/s10562-009-0217-3

A Simple Method for Synthesis of S-Doped TiO_2 of High Photocatalytic Activity

Priyanka P. Bidaye · Deepa Khushalani · J. B. Fernandes

Received: 18 September 2009 / Accepted: 4 November 2009 / Published online: 18 November 2009
© Springer Science+Business Media, LLC 2009

Abstract S-doped TiO_2 samples were synthesized by use of thiourea. The elemental analysis was confirmed by X-ray fluorescence, the phases were identified by X-ray diffraction and further characterization was carried out by surface area measurement and UV–Vis spectroscopy. The photocatalytic activity was measured by exposing methylene blue to sunlight in the presence of TiO_2. It was observed that the S-doped anatase phase showed high photocatalytic activity in comparison to other samples.

Keywords S-TiO_2 · Anatase · Rutile · Photocatalytic degradation · Methylene blue

1 Introduction

TiO_2 is a highly investigated photocatalyst, however its application is limited in the UV region due to the large band gap value of 3.2 eV. Several attempts have been made to shift its photoresponse in the visible region. One approach is to dope TiO_2 by transition metals [1, 2] and another has been to form reduced TiO_x photocatalysts [3, 4]. It was shown that the optical response of TiO_2 could be shifted from UV to visible region by doping with non metal atoms such as N, C, S, I, P, F, B [5–9].

Although Asahi et al. [5] predicted that the doping of N or S would be most effective in non metal doped TiO_2, the S ion was hard to be introduced in TiO_2 matrix due to its large ionic radius. Umebayashi et al. [7] successfully synthesized S-doped TiO_2 by oxidation annealing of TiS_2 in which S atoms replaced O atoms and the S doped TiO_2 showed optical absorption red shift. The electronic structure analysis attributed the band gap narrowing to the S 3p states on the upper edge of the valence band [10, 11]. Later Ohno et al. [12, 13] prepared S cation doped TiO_2, having high photoactivity in the visible region in which S atoms substituted for Ti.

The rutile and anatase phases dominate for the low S-doped and high S-doped TiO_2 nanoparticles, respectively. The variation of phase with different S doping levels has been ascribed to the different S doping processes into TiO_2 nanoparticles [14]. In previous reports, S doped TiO_2 photocatalysts have been mainly prepared by calcining materials containing titanium at high reaction temperatures [7, 13]. Li et al. [15] reported that Sulphur could be doped into titania by treating TiO_2 precursor (xerogel) under supercritical conditions in CS_2/ethanol fluid at 280 °C. Nanometer films of S doped TiO_2 have been prepared by sol–gel method using alkoxides and are studied for chlorobenzene removal [16]. Wei et al. have succeeded in synthesizing doped anatase TiO_2 with good crystallinity by one step hydrothermal method from a mixed aqueous solution of $Ti(SO_4)_2$ and thiourea [17].

The S-TiO_2 photocatalysts prepared by using tetrabutyl titanate in alcohol have been studied for decomposition of methylene blue [18] and L-acid [19]. S-doped TiO2 photocatalyst with high activity for phenol degradation under

Electronic supplementary material The online version of this article (doi:10.1007/s10562-009-0217-3) contains supplementary material, which is available to authorized users.

P. P. Bidaye · J. B. Fernandes (✉)
Department of Chemistry, Goa University, Taleigao Plateau, Goa 403206, India
e-mail: juliofernandes@rediffmail.com

D. Khushalani
Tata Institute of Fundamental Research, Homi Bhabha Road, Colaba, Mumbai 400005, India

visible light has been synthesized by acid catalyzed hydrolysis of $TiCl_4$, using thiourea as the source of S [20].

Hydrothermal treatment of aqueous solutions of $TiCl_4$ and thiourea have been recently employed at a relatively low temperature of 180 °C to synthesize nanocrystalline S doped TiO_2 having excellent photocatalytic activities for degradation of methyl orange [21]. However $TiCl_4$ is difficult to handle as it fumes easily. The use of alkoxide in synthesis warrants tight control of experimental conditions like pH, humidity etc. because of the intense hydrolysis of the alkoxide in air. The high cost of alkoxide limits commercialization of such process. It is also reported that the TiO_2 synthesized using titanium sulphate is comparatively less active [22]. Use of organic solvents and autoclave as a reactor makes the synthesis process difficult and expensive at industrial scale.

We report herein a relatively simple method to synthesise photoactive 'S' doped TiO_2 with high surface area, using $TiCl_3$ as the precursor and thiourea as the source of S.

2 Experimental

2.1 Catalyst Preparation

The catalysts were synthesized by dropwise addition of 0.5 M HNO_3 to a 15% $TiCl_3$ solution until its colour changed from violet to colourless. This was followed by the addition of oxalic acid and thiourea such that the $TiCl_3$: oxalic acid: thiourea, molar ratio in the final solution was 1:0:2 for R2 and 1:1:2 for R3. The blank sample R1 was synthesized by dropwise addition of 0.5 M HNO_3 to a 15% $TiCl_3$ solution until colourless. The resultant solutions were evaporated to dryness on a steam bath. A small portion of the dry precursor was first analysed by TG/DSC studies in order to select the synthesis temperature. The residue was then heated in a muffle furnace at 450 °C for 4 h for R1, R2 and 6 h for R3 to obtain the final sample.

2.2 Catalyst Characterization

The X-ray powder diffraction patterns (XRD) have been recorded on a Shimadzu LabX-700 diffractometer, using Ni filtered Cu Kα radiation ($\lambda = 1.5406$ Å). The Scherrer crystallite sizes were determined using the formula $t = 0.9\lambda/\beta\cos\theta$ where λ is the wavelength characteristic of the Cu Kα radiation, β is the full width at half maximum (in radians) and θ is the angle at which 100 intensity peak appears. The weight percent of anatase in the rutile phase was obtained from the below equation [23]

$$X_A = [1 + 1.26(I_R/I_A)]^{-} \times 100$$

where X_A is the weight fraction of anatase in the mixture, I_R and I_A were obtained from the peak areas of rutile (110) and anatase (101) diffractions, respectively.

Nitrogen adsorption and desorption isotherms were obtained with a Micrometrics Tristar 3000 surface area and porosity analyzer.

Thermogravimetric analysis (TGA) and differential thermal analysis (DTA) of precursors were carried out on Shimadzu DTG-60 thermal analyzer.

The absorption edges and band gaps were determined from the onset of diffuse reflectance spectra of the samples measured using UV–VIS spectrophotometer (Shimadzu UV-2450). The presence of Sulfur was confirmed from S binding energy peaks in XRF spectra that was carried out on JEOL JSX-3222 spectrometer.

3 Results and Discussions

3.1 Catalyst Characterization

Figure 1 gives the XRD patterns of the samples. The sample R2 prepared by calcination of acidified $TiCl_3$ in presence of thiourea showed mixed phase of anatase and rutile. On the other hand R3 prepared by additional use of 1 mol oxalic acid was pure anatase. Table 1 summarizes the crystal phase of the samples in relation to other physico-chemical parameters. As evident from Table 1, all the samples were nanocrystalline with the crystallite sizes in the range 12–14 nm, while the surface areas were in the range 42–67 m^2/g. It is observed that TiO_2 synthesized by additional presence of oxalic acid shows 100% anatase phase while the mixed phase is observed in samples synthesized without the addition of oxalic acid.

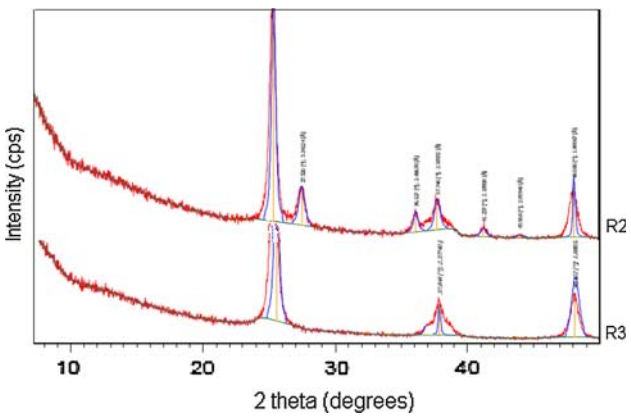

Fig. 1 X-ray diffraction profiles of synthesized TiO_2 samples R2 (rutile + anatase mixed phase) and R3 (anatase)

Table 1 Structural properties of titania samples

Sr. no.	Code	Method	Phase (% anatase)	Scherrer crystallite sizes	BET surface area (m^2/g)	Pore volume (cm^3/g)	Pore diameter (nm)
1	R1	$TiCl_3$: HNO_3	52	14	42	0.13	9.32
2	R2	$TiCl_3$ (HNO_3): Thiourea (1:2)	82	13	66	0.17	11.32
3	R3	$TiCl_3$(HNO_3): Thiourea: Oxalic acid (1:2:1)	100	12	67	0.16	8.16

Figure 2 gives the XRF spectra that confirms the presence of Sulfur binding energy peak, however no Nitrogen peak was observed.

Figure 3 shows SEM images of R2 and R3, respectively, which clearly shows spherical agglomerates of numerous nanoparticles.

The N_2 adsorption–desorption isotherms for the synthesized samples R1, R2 and R3 are as given in Fig. 4a, b and c, respectively. Shapes of isotherms showed a typical type III isotherm [24]. Presence of H3 type hysterisis loops for these isotherms suggested the formation of slit shaped pores in the mesopore range. A clear hysterisis at high relative pressure is observed, which is related to capillary condensation associated with large pore channels. The surface area and pore size parameters as calculated from the desorption branch of the isotherm as shown in Table 1. Average pore diameter of all the samples was in mesoporous range (8–12 nm). The samples showed two categories of pore size distribution

(1) narrow pore size distribution with most of the pores centered at ~4 nm.
(2) a broad 'hill' in the mesoporous range of 5–20 nm.

The pore size distribution of all the samples thus confirm the mesoporosity of all the samples. The *t*-plot of all the samples indicated the presence of only mesopores and no micropores in all the samples.

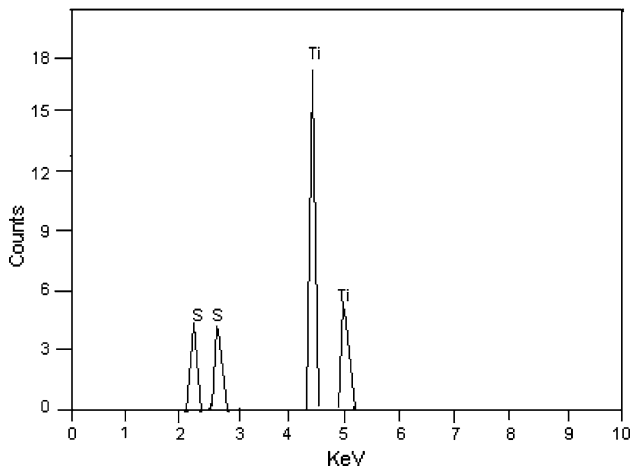

Fig. 2 X-ray fluorescence spectrum of synthesized TiO_2 sample R2 prepared using $TiCl_3$, HNO_3 and thiourea

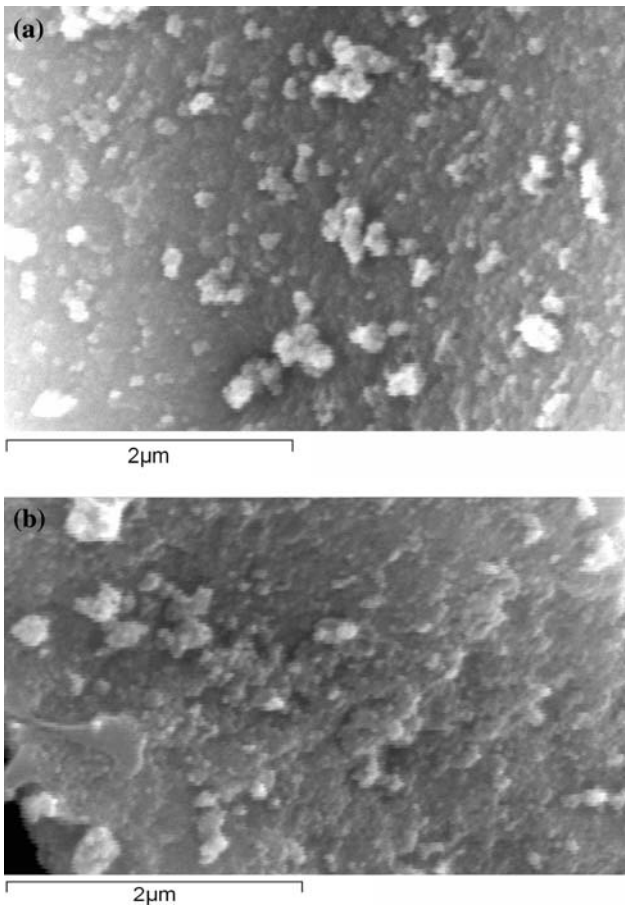

Fig. 3 SEM images of the TiO_2 samples. **a** sample R2 and **b** sample R3

3.2 Phase Formation and Photocatalysis

The precursor for R1 i.e., $TiCl_3$ acidified with HNO_3 when dried on a steam bath, appeared semisolid non sticky yellow mass. On the other hand the precursor for R2 viz. the mixture of $TiCl_3$, HNO_3 and thiourea when similarly treated, appeared hygroscopic and formed a kind of semisolid yellow sticky mass. However the precursor for R3 which is a mixture of $TiCl_3$, HNO_3, thiourea and oxalic acid appeared as an amorphous, fluffy white powder.

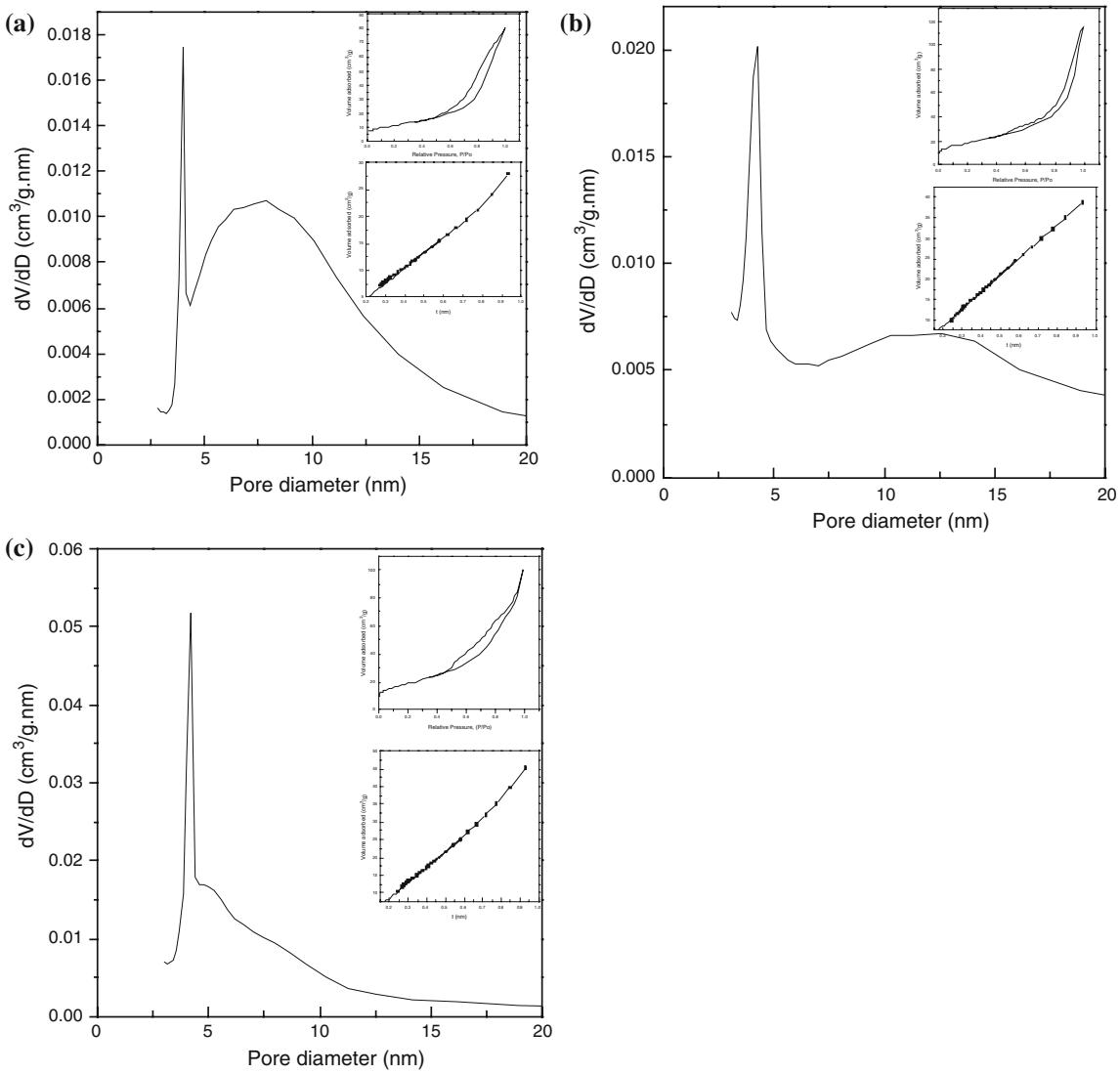

Fig. 4 **a** N_2 adsorption–desorption isotherms and BJH analysis for R1. **b** N_2 adsorption–desorption isotherms and BJH analysis for R2. **c** N_2 adsorption–desorption isotherms and BJH analysis for R3

Similar observation was reported during the synthesis of N-doped anatase phase when urea was used in place of thiourea [25]. It is also evident from Table 1 that the use of oxalic acid during the synthesis favoured the formation of anatase phase.

To investigate the oxidative decomposition behaviour of the precursors, TGA-DTA analysis was carried out. Figure 5 gives example of a typical thermogram of the precursor prepared by using $TiCl_3$, HNO_3 and thiourea.

It was observed that ~8% weight loss occurred in the temperature range 30–150 °C due to elimination of water from the precursor gel. Further in the temperature range of 150–250 °C, weight loss of ~60% has been observed. The DTA profile showed the corresponding endothermic peak in this temperature range. This is attributed to the dehydration of the sample followed by combustion of the

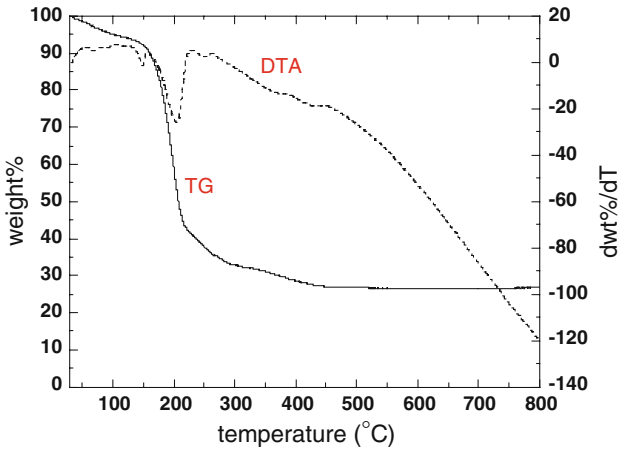

Fig. 5 Thermogravimetric and differential thermal analysis curves of the precursor for R2

Table 2 The calculated band gaps of the as prepared titania samples

Catalyst	R1	R2	R3	Degussa P-25
Band gap (eV)	3.09	2.43	3.03	3.14

organic matter. Also a weight loss of ~12% was observed in the temperature range of 250–450 °C. However heating the sample beyond 450 °C, did not produce any weight loss steps and energy changes, thus confirming the transformation of the precursor into TiO_2 (Table 2).

Figure 6 shows the diffuse reflectance spectra of the Titania samples. It is clear that all these samples showed absorption edge in the visible region. The band gap of the samples was determined by the equation $Eg = 1{,}239.8/\lambda$ [26], where Eg is the band gap energy (eV) and λ (nm) is the wavelength of the absorption edges in the spectra.

The photocatalytic activity of S doped TiO_2 was investigated for the degradation of Methylene Blue (MB) dye

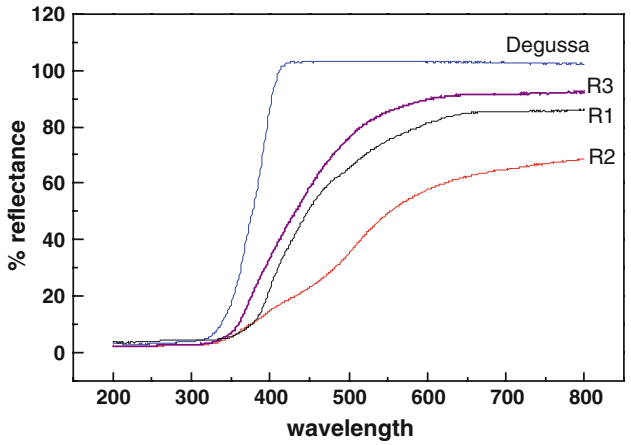

Fig. 6 Diffuse reflectance spectra of the catalysts R1, R2, R3 and commercial degussa P-25

($<10^{-5}$ M) at 660 nm as per the procedure reported earlier [19]. The experiments were carried out simultaneously for all the catalysts in bright sunlight, between 10.00 a.m. and 12.00 noon. Experiments were repeated for all the catalysts simultaneously on three different days in order to confirm consistency of results. In a typical run 50 mL of aqueous dye solution and 0.2 g of the catalyst was exposed to sunlight for the duration of the experiment. The solutions thus exposed to sunlight were stirred intermittently. After every 30 min, 2 mL aliquots were pipetted out, centrifuged and the absorbance of the clear supernatants was determined at 660 nm wavelength for methylene blue, against appropriate blanks. The resulting profiles are shown in Fig. 7.

The inset figure shows the expected time dependent spectra as decolorisation of methylene blue proceeds. It is clear from the Figure that the anatase TiO_2 catalyst R3 as expected showed highest photocatalytic activity and was quite comparable to that of Degussa P 25. This was followed by samples R2 and R1 as the presence of anatase phase decreased in these samples. However both the S-doped rutile as well as S-doped anatase showed higher photocatalytic activity than the undoped rutile catalyst. It may be noted that both these S-doped samples showed similar crystallite sizes and surface areas (~67 m^2/g). However the band gap in R2 being lower (2.43 eV) than that in R3 (3.03), it is possible that the higher rate of electron–hole recombination in R2 resulted in relatively lower activity than the S-doped anatase phase.

4 Conclusions

(1) A nanocrystalline S-doped TiO_2 has been synthesized by a simple method involving $TiCl_3$, HNO_3 and thiourea
(2) Use of oxalic acid during synthesis resulted in the formation of anatase phase

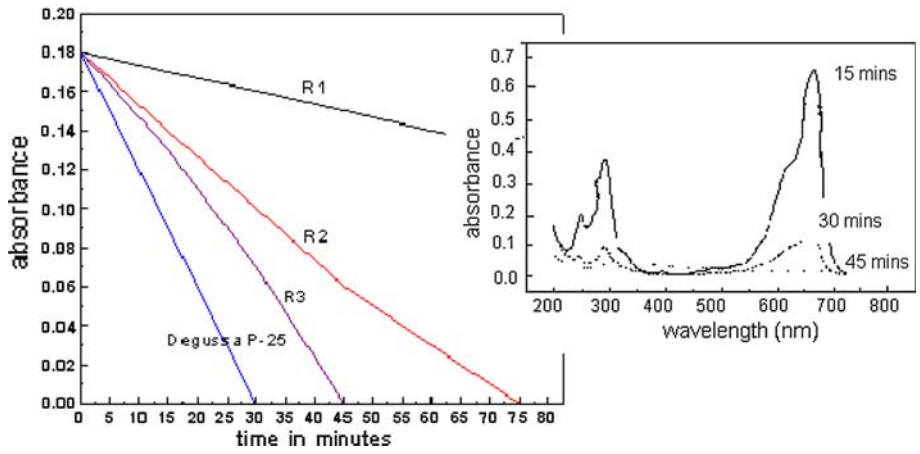

Fig. 7 Photocatalytic degradation profiles of the TiO_2 catalysts R1, R2, R3 and degussa P-25 for degradation of Methylene Blue

(3) Both the S-doped rutile and S-doped anatase showed higher photocatalytic activity as compared to the undoped TiO_2
(4) The relatively low activity of S-doped rutile as compared to S-doped anatase is attributed to higher rate of electron–hole recombination in the former

Acknowledgments The authors are grateful for the financial support received vide UGC-SAP F.540/25/DRS/2007 (SAP-II). The authors also convey thanks to Mr. Bhanudas Naik and Dr. N. N. Ghosh, Assistant Professor, BITS-Pilani, Goa Campus for their help in various ways.

References

1. Ghosh AK, Maruska MP (1977) J Electrochem Soc 124:1516
2. Choi W, Termin A, Hoffmann MR (1994) J Phys Chem 98:13669
3. Breckenridge RP, Hosler WR (1953) Phys Rev 91:793
4. Cronemeyer DC (1959) Phys Rev 113:1222
5. Asahi R, Morikawa T, Ohwaki T, Aoki K, Taga Y (2001) Science 293:269
6. Khan SUM, Al-Shahry M, Ingler WB (2002) Science 297:2243
7. Umebayashi T, Yamaki T, Itoh H, Asai K (2002) Appl Phys Lett 81:454
8. Yu JC, Zhang LZ, Zheng Z, Zhao JC (2003) Chem Mater 15:2280
9. Yin S, Ihara K, Komatsu M, Zhang QW, Zhang F, Kyotani T, Sato T (2006) Solid State Commun 137:132
10. Tian FH, Liu CB (2006) J Phys Chem B 110:17866
11. Cui Y, Du H, Wen L (2009) Solid State Commun 49:634
12. Ohno T, Mitsui T, Matsumura M (2003) Chem Lett 32:364
13. Ohno T, Akiyoshi M, Umebayashi T, Asai K, Mitsui T, Matsumura M (2004) Appl Catal A 265:115
14. Wu XW, Wu DJ, Liu XJ (2009) Appl Phys A- Mat Sci and Process 97:248
15. Li HX, Zhang XY, Huo YN, Zhu J (2007) Environ Sci Techno 41:4410
16. Crisan M, Braileanu A, Raileanu M, Zaharescu M, Crisan MD, Dragan N, Anatasesue M, Janculescu A, Nitoi I, Marinescu VE, Hodorogea SM (2008) J Non Crystalline Solids 354:705
17. Wei F, Ni L, Cui P (2008) J Hazard Mater 156:135
18. Zhang S, Song L, Zhang S, Donglan S, Chen B (2009) React Kinet Catal Lett 97:199
19. Wang Y, Li J, Peng P, Lu T, Wang L (2008) Appl Surf Sci 254:5276
20. Liu S, Chen X (2008) J Hazard Mater 152:48
21. Tian H, Ma J, Li K, Li J (2009) Ceram Intern 35:1289
22. Gandhe AR, Naik SP, Fernandes JB (2005) Microporous Mesoporous Mater 87:103
23. Spurr RA, Myers H (1957) Anal Chem 29:760
24. Sing KSW, Everett DH, Haul RAW, Moscou L, Pierotti RA, Rouquerol J, Siemienie Wska T (1985) Pure and Appl Chem 57:603–604
25. Gandhe AR, Fernandes JB, Varma S, Gupta NM (2005) J Mol Catal A Chem 238:63
26. Regan BO, Gratzel M (1991) Nature 353:737l